Radiation dose reduction in digital breast tomosynthesis (DBT) by means of deep-learning-based supervised image processing

Liu, Junchi, Zarshenas, Amin, Qadir, Ammar, Wei, Zheng, Yang, Limin, et al.

Junchi Liu, Amin Zarshenas, Ammar Qadir, Zheng Wei, Limin Yang, Laurie Fajardo, Kenji Suzuki, "Radiation dose reduction in digital breast tomosynthesis (DBT) by means of deep-learning-based supervised image processing," Proc. SPIE 10574, Medical Imaging 2018: Image Processing, 105740F (2 March 2018); doi: 10.1117/12.2293125

SPIE.

Event: SPIE Medical Imaging, 2018, Houston, Texas, United States

Radiation dose reduction in digital breast tomosynthesis (DBT) by means of deep-learning-based supervised image processing

Junchi Liu, M.S.*[a], Amin Zarshenas, M.S.[a], Ammar Qadir, B.S.[a], Zheng Wei, M.S.[a], Limin Yang, M.D., Ph.D.[b], Laurie Fajardo, M.D., M.B.A.[c], Kenji Suzuki, Ph.D.[a]

[a] Computational Intelligence in Biomedical Imaging Lab, Dept. of Electrical and Computer Engineering, Illinois Institute of Technology, 10 West 35th Street, Chicago, IL, USA 60616-3793; [b]Dept. of Radiology, Univ. of Iowa Hospitals and Clinics, 200 Hawkins Drive, Iowa City, IA, USA 52242-1077; [c]Dept. of Radiology and Imaging Sciences, Univ. of Utah, 30 North 1900 East, Salt Lake City, UT, USA 84132-2140

ABSTRACT

To reduce cumulative radiation exposure and lifetime risks for radiation-induced cancer from breast cancer screening, we developed a deep-learning-based supervised image-processing technique called neural network convolution (NNC) for radiation dose reduction in DBT. NNC employed patched-based neural network regression in a convolutional manner to convert lower-dose (LD) to higher-dose (HD) tomosynthesis images. We trained our NNC with quarter-dose (25% of the standard dose: 12 mAs at 32 kVp) raw projection images and corresponding "teaching" higher-dose (HD) images (200% of the standard dose: 99 mAs at 32 kVp) of a breast cadaver phantom acquired with a DBT system (Selenia Dimensions, Hologic, Inc, Bedford, MA). Once trained, NNC no longer requires HD images. It converts new LD images to images that look like HD images; thus the term "virtual" HD (VHD) images. We reconstructed tomosynthesis slices on a research DBT system. To determine a dose reduction rate, we acquired 4 studies of another test phantom at 4 different radiation doses (1.35, 2.7, 4.04, and 5.39 mGy entrance dose). Structural SIMilarity (SSIM) index was used to evaluate the image quality. For testing, we collected half-dose (50% of the standard dose: 32±14 mAs at 33±5 kVp) and full-dose (standard dose: 68±23 mAs at 33±5 kvp) images of 10 clinical cases with the DBT system at University of Iowa Hospitals & Clinics. NNC converted half-dose DBT images of 10 clinical cases to VHD DBT images that were equivalent to full-dose DBT images. Our cadaver phantom experiment demonstrated 79% dose reduction.

Keywords: deep learning, radiation dose reduction, patched-based neural network, virtual high-dose technology

1. INTRODUCTION

Breast cancer is the most common cancer except for skin cancers and the second leading cause of cancer death among women in the U.S.[1]. Mammography has been used in screening for breast cancer[2]. The goal of screening mammography is the early detection of breast cancer through detection of suspicious masses, architectural distortion and microcalcifications. There are three known limitations associated with mammography screening: (1) false positive results (high recall rates), (2) false negative results, and (3) radiation exposure. The ten-year cumulative risk of a false-positive biopsy result in annual mammography screening is 7%[3]. A significant, if not the main, cause of false-negative results is high breast density that obscures breast tumors in 2D projection mammograms[4].

To improve the issues of false positives and negatives, digital breast tomosynthesis (DBT)[5],[6] was developed. DBT is a 3D imaging technology that takes multiple projections over a limited angle range to reconstruct a 3D volume of image slices. An advantage of DBT over conventional 2D mammography for breast cancer screening and diagnostic mammography is that DBT reduces the problem of tissue overlap in a 2D projection mammogram and improves lesion conspicuity especially for dense breasts. DBT has shown to be a promising modality for early detection of breast cancer, with higher cancer detection rates and fewer patient recalls (false positives)[5],[7]-[9].

*jliu118@hawk.iit.edu; phone 1 312 647-4001; Computational Intelligence in Biomedical Imaging Lab; http://www.ece.iit.edu/~ksuzuki/members/junchi-liu-m-s/

Medical Imaging 2018: Image Processing, edited by Elsa D. Angelini, Bennett A. Landman, Proc. of SPIE
Vol. 10574, 105740F · © 2018 SPIE · CCC code: 1605-7422/18/$18 · doi: 10.1117/12.2293125

With digital DBT, a remaining major challenge in breast cancer screening is radiation exposure. The FDA approved two scenarios with DBT: 1) DBT combined with conventional full-field digital mammography (FFDM) and 2) DBT with "synthesized" 2D mammograms obtained from a 3D DBT volume. In the two scenarios, the radiation dose (5-8 mGy)[10] to the radiosensitive breasts in DBT can be 1.4-2.3 times higher than the conventional 2D digital mammography radiation dose (about 3.5 mGy). Repeated DBT for annual screening could increase cumulative radiation exposure and lifetime attributable risks for radiation-induced breast cancer. A recent study conducted by Drs. Martin Yaffe and James Mainprize estimated that 11 deaths from 86 radiation-induced breast cancers would occur within a cohort of 100,000 women each receiving a dose of 3.7 mSv during annual mammographic screening. Based on the study results for mammography screening, repeated DBT with FFDM annual screening of women starting at age 40 years could cause one life lost due to radiation-induced cancer per 18.9-47.4 lives saved[11],[12]. Therefore, radiation dose reduction is crucial for breast cancer screening with DBT.

To reduce the radiation dose in DBT, a technique that creates a 2D synthesized image from 3D image slices was developed to eliminate the necessity of separate acquisition of a 2D mammogram. However, Yaffe[13] pointed out that even with use of the 2D synthetic image, radiation dose from 3D breast tomosynthesis can still be an issue, because radiation dose of 3D breast tomosynthesis can be higher than that of 2D mammography. In fact, the radiation dose by DBT with a 2D "synthetic" mammogram (5 mGy)[10] can still be 1.4 times higher than a typical mammography radiation dose. Although noise reduction techniques such as block-matching 3D (BM3D)[14] and dictionary learning[15] may be used for radiation dose reduction in DBT, they tend to smooth out image details and subtle patterns such as microcalcifications. It is difficult to achieve an optimal tradeoff between structure preservation and noise reduction by these techniques. In addition, they may not reduce artifact. Thus, it is a challenge to reduce noise and artifact in DBT while maintaining important diagnostic information and depiction of subtle lesions.

In this paper, we propose a supervised image-processing technique based on NNC[16] for radiation dose reduction in DBT. NNC is a supervised patch-based machine learning technique consisting of a neural network regression model. Our NNC converts LD images to "virtual" HD images where noise and artifact in the LD images are significantly reduced, while maintaining breast tissue and subtle structures such as tiny microcalcifications. To our knowledge, there is no deep-learning technique[17] that has been developed for radiation dose reduction in DBT. In contrast to typical deep-learning techniques that output class labels, NNC is able to directly learn and output desired images. We trained and validated our dose reduction technology with breast cadaver phantoms acquired at different radiation dose levels with a DBT system (Selenia Dimensions, Hologic, MA). The SSIM index[32] was employed to evaluate the image quality. In addition, we compared the performance of our NNC with ones of the best-known noise reduction techniques, namely, bilateral filtering[33], BM3D[14] and K-SVD[15]. To further evaluate the robustness and performance of our technology, we applied our trained NNC on 10 clinical cases.

2. MATERIALS AND METHODS

1 Basic principles of our radiation dose reduction technology

Figure 1 and Figure 2 illustrate the basic principle of our technology for radiation dose reduction in DBT. Our NNC consists of a neural network regression model with patch input. The output of NNC is single pixels. To obtain the entire image, our NNC scans over the input images in a convolutional manner. NNC is trained with LD images and corresponding "teaching" HD images of a breast phantom, as shown in Figure 1. Through the training, the NNC learns the relationship between the input LD images and the teaching HD images to convert LD images with abundant noise and artifacts due to low radiation exposure into HD images with less noise or artifacts. In the testing phase, our NNC no longer requires HD images. The trained NNC model is applied to new LD images to produce the images similar to HD images where noise and artifacts are substantially reduced, as shown in Figure 2.

2 Architecture of NNC

In the field of image processing, Suzuki et al. developed supervised nonlinear filters and edge enhancers based on a neural network (NN), called neural filters[18],[19] and neural edge enhancers[20],[21], respectively, which are considered early contributions to the field of deep learning. In the domain of computer-aided diagnosis (CAD), Suzuki et al. invented a massive-training artificial NN (MTANN) by extending neural filters and edge enhancers to accommodate pattern-recognition and classification tasks[22]-[26]. In this study, we extended MTANNs and developed a general framework for supervised image processing, called a machine-learning convolution. An NNC consists of a linear-output-

layer neural network (NN) regression (LNNR) model[20] which is capable of deep layers. The NNC can be considered as a supervised nonlinear filter that can be trained with input images and the corresponding "teaching" images. The LNNR model, which is capable of operating on image data directly, employs a linear function instead of a sigmoid function in the output layer because the characteristics of an NN were improved significantly when applied to the continuous mapping of values in image processing[20]. The NNC model consists of an input layer, a convolutional layer, multiple fully-connected hidden layers, and an output layer. The input layer of the LNNR receives the pixel values in a 2D subregion (or kernel, image patch), R, extracted from input LD images. The output $O(x,y)$ of the NNC is a continuous value, which corresponds to the center pixel in the sub-volume (or image patch), represented by

$$\hat{g}(x,y) = NN\{f(x-i,y-j)\,|\,(i,j)\in R\}, \quad (1)$$

where $NN\{\cdot\}$ is the output of the LNNR model, $f(x,y)$ is the normalized input pixel value, and $\hat{g}(x,y)$ is an estimate of a desired/ideal value. Note that only one unit is employed in the output layer. Other machine-learning models such as support vector regression and nonlinear Gaussian process regression[27] can be used instead of the LNNR model, which forms a machine-learning convolution. The entire image is obtained by scanning the LNNR model in a convolutional manner, thus the term NNC. For training to convert input LD images with noise and artifacts into desired VHD images, we define the error function to be minimized, represented by

$$\varepsilon = \frac{1}{P}\sum_{(x,y)\in R_T}\{g(x,y)-\hat{g}(x,y)\}^2, \quad (2)$$

where R_T is a training region, $g(x,y)$ is the "teaching" desired image and P is the number of training samples. The NNC is trained by a linear-output-layer back-propagation (BP) algorithm[20], which is a backpropagation algorithm modified for the LNNR model[30]. After training, the NNC is expected to output the values close to desired pixel values in the teaching images. Thus, the trained NNC would convert new LD images to VHD images without requiring HD images.

3 Training and validation with breast cadaver phantom

To train and validate our radiation dose reduction technology based on NNC, we acquired 5 studies at different radiation dose levels of two breast cadaver phantoms with a DBT system (Selenia Dimensions, Hologic, Inc, Bedford, MA). The radiation doses were altered by changing tube current-time product, while the tube voltage was fixed at 33 kVp. The tube current-time products, the corresponding tube currents, and the corresponding entrance dose in the acquisitions were as follows: 12, 24, 36, 52, and 99 mAs; 80, 165, 190, 190, and 190 and 133 mA; 1.35, 2.71, 4.04, 5.78 and 11.06 mGy, respectively. The tube current-time product of 52 mAs is considered the standard dose for the particular breast phantoms. Thus, the acquisitions were approximately 25, 50, 75, 100, and 200% of the standard dose. The spatial resolution (pixel size) of reconstructed slices was 0.117 mm/pixel and the matrix size of an image was 1996×2457 pixels with the slice thickness of 0.9 mm. NNC was trained with an input lower-dose (12 mAs, 32 kVp, 1.35 mGy in entrance dose, 25% of the standard dose) raw projection images of each of the two breast phantoms and the corresponding higher-dose (99 mAs, 32 kVp, 200% of the standard dose) raw projection images. NNC could be trained with only one case, because a large number of training image patch samples was extracted from the case and used for training[31]. Each of the trained NNCs was applied to a non-training low-dose (12 mAs, 32 kVp, 1.35 mGy in entrance dose, 25% of the standard dose) raw projection image of the other breast phantom so that training and testing were completely separated.

We evaluated the dose reduction performance by measuring the structural similarity (SSIM) index between the phantom VHD raw-projection images and the corresponding HD raw-projection images. Inputs of the NNC were quarter-dose tomosynthesis raw-projection images. SSIM is a widely accepted image quality measure that overcomes the limitation of conventional contrast/signal-to-noise-ratio (CNR or SNR) with lack of spatial information (e.g., structure) in evaluation. The SSIM index is represented by

$$SSIM(x,y) = \frac{(2\mu_x\mu_y + C_1)(2\sigma_{xy} + C_2)}{(\mu_x^2 + \mu_y^2 + C_1)(\sigma_x^2 + \sigma_y^2 + C_2)}, \quad (3)$$

where μ_x, μ_y, σ_x, σ_y, $\sigma_{x,y}$ are the local means, standard deviations, and cross-covariance for images x, y. $C_1 = (k_1 L)^2, C_2 = (k_2 L)^2$, where L is the dynamic range of the pixel values, k_1 and k_2 are constants[32].

4 Clinical case evaluation

For further evaluation of our technology, we collected half-dose (50% of the standard dose) and full-dose (100% of the standard dose) DBT images of 10 clinical cases with a DBT system (Selenia Dimensions, Hologic) at University of Iowa Hospitals & Clinics. The half-dose DBT images were obtained by changing tube current-time product, while the tube voltages were at 33±5 kVp. Tube current, tube current-time product, and entrance dose for full-dose DBT images were 180±20 mA, 68±23 mAs, and 9.27±6.31 mGy, respectively, whereas those for half-dose DBT images were 163±38 mA, 32±14 mAs, and 4.55±3.30 mGy, respectively. The spatial resolution (pixel size) of reconstructed slices was 0.106±0.011 mm/pixel and the matrix size of an image was 1996×2457 or 1890×2457 pixels with the slice thickness of 0.88±0.05 mm. We applied our trained NNC to the half-dose images to produce VHD images.

3. RESULTS

1 Breast cadaver phantom study

Our trained NNC was able to convert quarter-dose images (1.35 mGy; SSIM: 0.88) of the testing cadaver phantom to VHD images with the image quality (SSIM: 0.97) equivalent to 119% dose images (6.41 mGy), thus it achieved 79% dose reduction, as shown in Figure 3. The SSIM value by our NNC exceeded the 100% dose SSIM value, because our NNC was trained with 200% dose images. In our VHD image, noise was suppressed, while maintaining the conspicuity of the clusters of tiny calcifications and vascular structures, as shown in Figure 4. The processing time for each study was 0.48 second on a GPU (GeForce GTX Titan Z, Nvidia, CA). We compared the performance of our NNC with ones of the best-known noise reduction techniques, namely, bilateral filtering, BM3D and K-SVD. The image quality of our VHD is superior to these of noise reduction technologies in terms of the SSIM values, as shown in Figure 5. The high SSIM value of our NNC indicates that NNC can not only substantially reduce noise but also achieve a better structure preservation performance of image details and subtle patterns such as tiny calcifications than that of the best-known noise reduction techniques.

2 Clinical case evaluation

To evaluate our technology further, we applied the trained NNCs to 10 clinical cases. Our NNC was able to convert half-dose clinical images to VHD images where noise was reduced while maintaining breast tissue structures and calcifications. We compared the VHD DBT images with corresponding "gold-standard" full-dose DBT images. The calcifications, breast masses and other breast-tissue structures in VHD images were equivalent to those in the corresponding full-dose images, as shown in Figure 6. In our VHD images, noise was reduced substantially, while maintaining the conspicuity of calcifications and breast tissue and vascular structures. The enlarged region shows the equivalent visualization of very small calcifications only 1.8 mm in size. The image quality of our VHD images obtained in half-dose acquisition is equivalent to that of real full-dose DBT images. Thus, our NNC achieved a 50% dose reduction rate.

4. CONCLUSION

Our radiation dose reduction technology based on NNC was able to convert LD DBT images to VHD DBT images which were equivalent to full-dose DBT images in the evaluation of 10 non-training clinical cases. It reduced noise in half-dose images, while preserving calcifications and breast-tissue structures. The time required to process each study on a GPU was 0.48 second. Our cadaver phantom experiments demonstrated a 79% radiation dose reduction rate. The performance of our NNC was superior to those of the best-known noise reduction technologies in terms of the SSIM values. Thus, substantial radiation dose reduction by our technology would benefit patients by reducing the risk of radiation-induced cancer from DBT screening.

ACKNOWLEDGEMENT

The authors are grateful to Ron Ho, Fred Ong, and Heather Rone (Alara Systems, CA) and Zhenxue Jing, Yiheng Zhang, and Jennifer Bartoshevich (Hologic, Bedford, MA) for their assistance and valuable discussions. This work was supported in part by a grant by Alara Systems, Inc., CA and an NIH grant (1U54TR002056) with University of Chicago Institute for Translational Medicine.

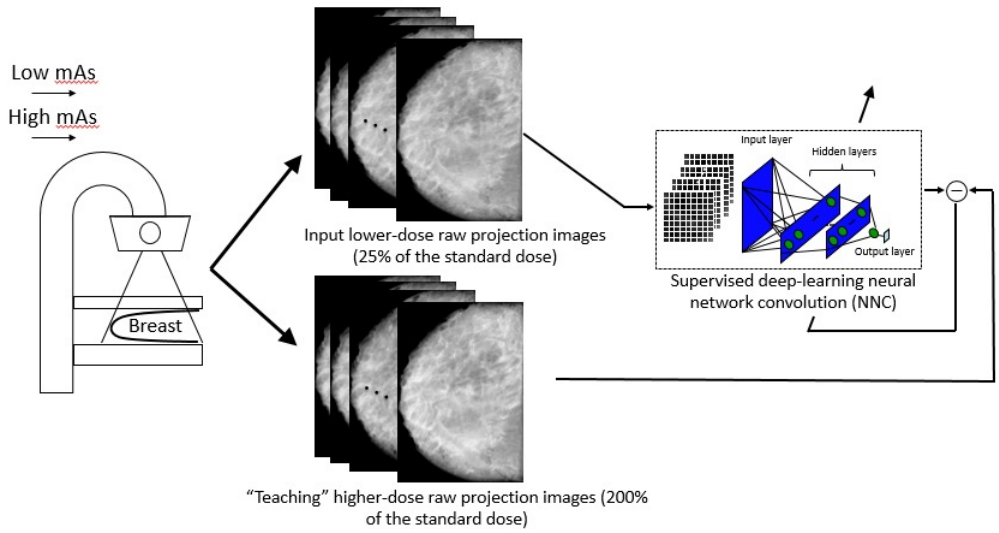

Figure 1. Training phase of NNC. NNC is trained with input quarter-dose images and the corresponding "teaching" higher-dose images.

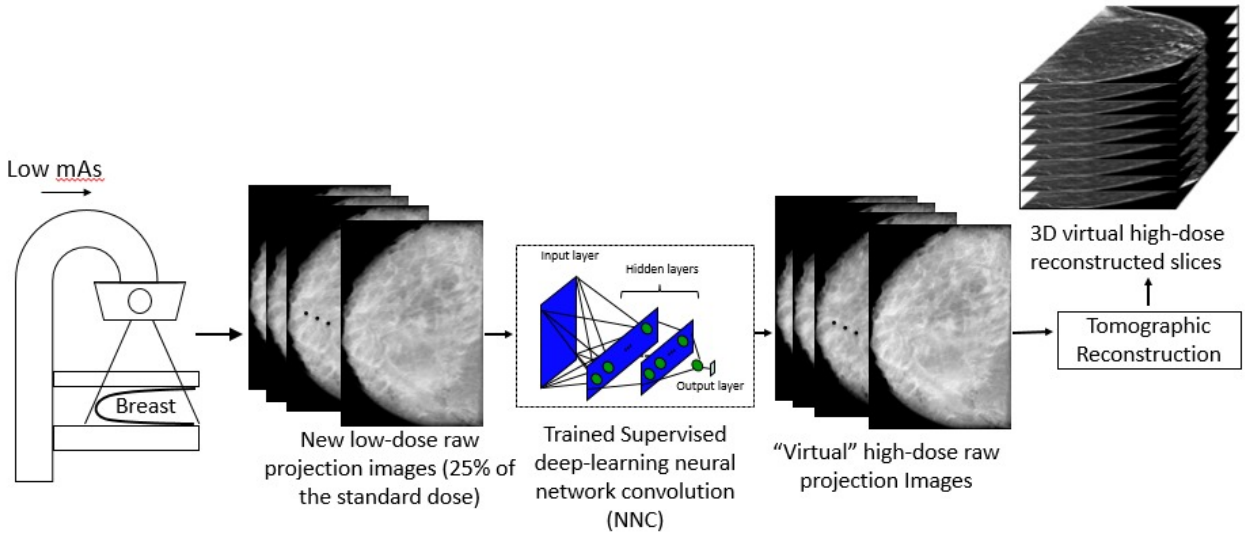

Figure 2. Testing phase of NNC. Once trained, our technique no longer requires higher-dose images. It applies to a new patient study to convert low-dose images to "virtual" high-dose images.

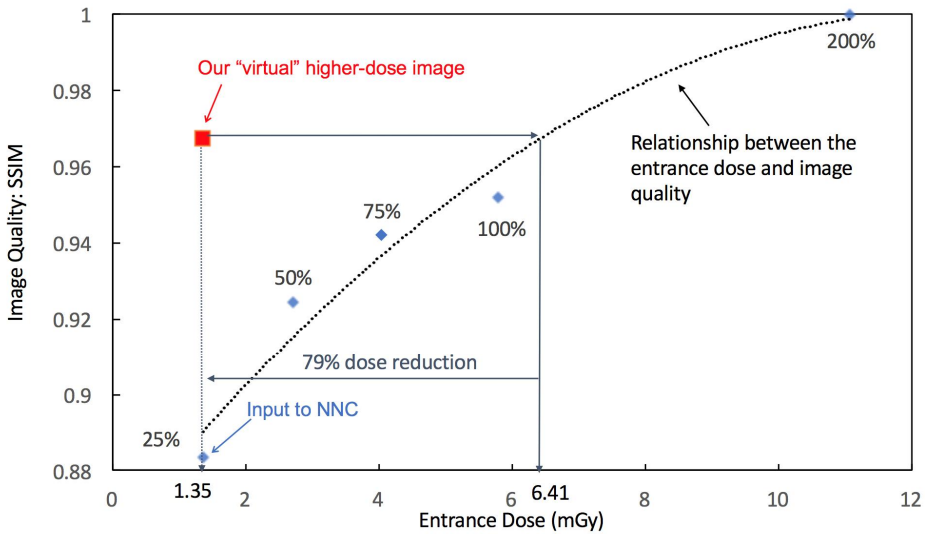

Figure 3. Estimation of radiation dose reduction by NNC from image quality measurement (SSIM: structural similarity index) in our breast cadaver phantom study.

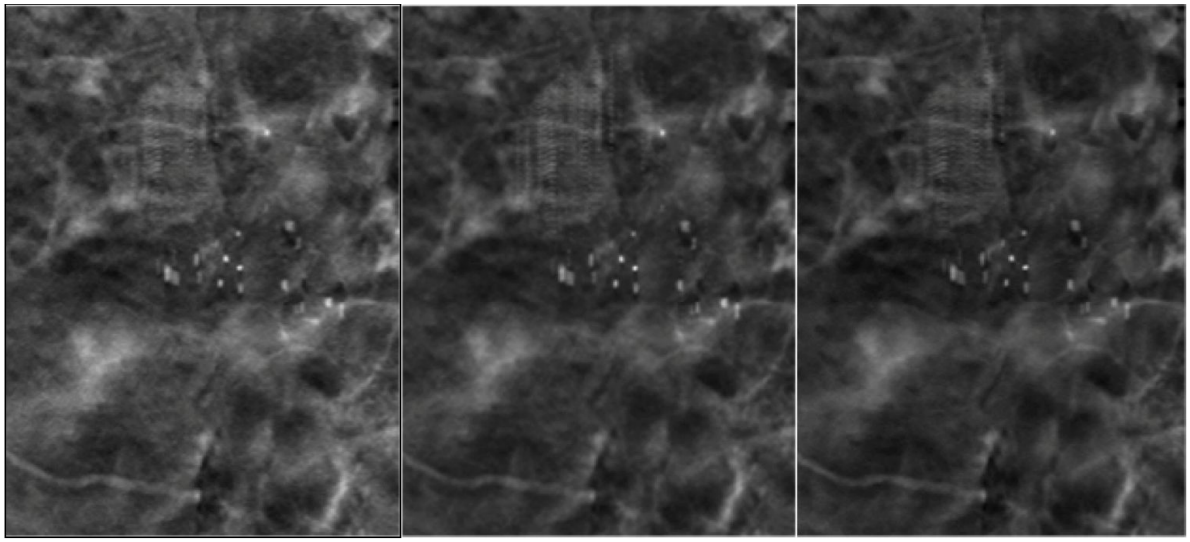

Original quarter-dose DBT slice (25% of standard dose) | Our virtual high-dose (VHD) DBT image for the quarter-dose slice (left) | "Gold-standard" real full-dose DBT slice (100% dose of standard dose)

Figure 4. Comparison of our VHD DBT image for one of cadaver phantom case with corresponding full-dose and quarter-dose DBT images. In our VHD image, noise was suppressed, while maintaining the conspicuity of the clusters of tiny calcifications.

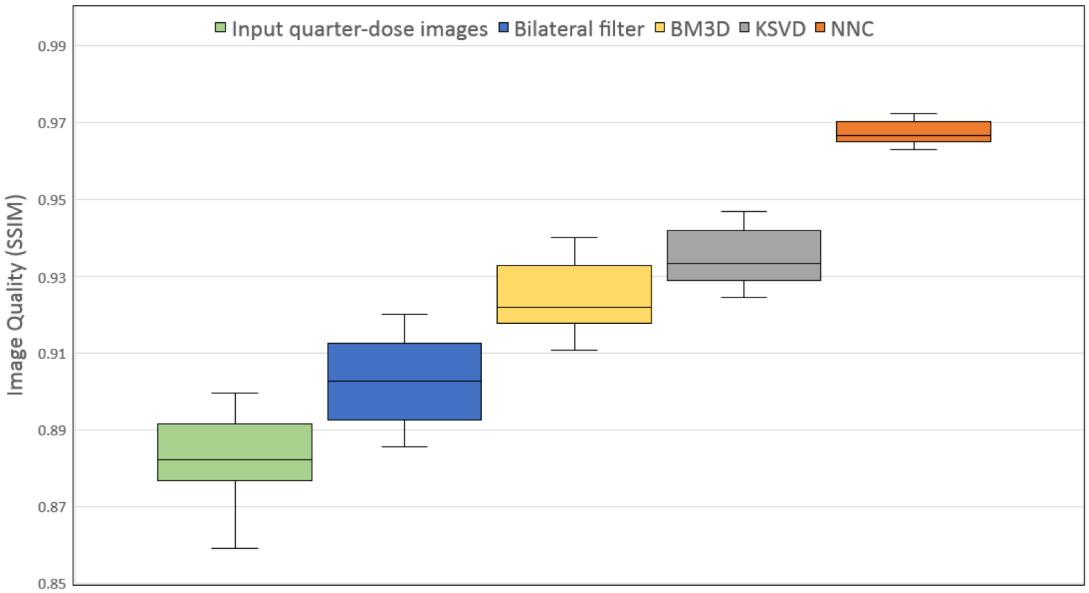

Figure 5. Performance comparison of our NNC with bilateral filtering, BM3D and KSVD in terms of SSIM in our breast cadaver phantom study.

Figure 6. Comparison of our VHD DBT image for one of 51 clinical cases with corresponding full-dose and half-dose DBT images. Breast calcifications were enlarged to show details. In our VHD images, noise is reduced substantially, while maintaining the conspicuity of calcifications and breast tissue and vascular structures. The image quality of our VHD images obtained in half-dose acquisition is equivalent to that of real full-dose DBT images.

REFERENCES

[1] Siegel RL, Miller KD, Jemal A., "Cancer statistics, 2016," CA Cancer J. Clin. 66(1), 7-30 (2016).
[2] Pisano ED, Gatsonis C, Hendrick E, et al. "Diagnostic performance of digital versus film mammography for breast-cancer screening," N Engl J. Med. 353, 1773- 83 (2005).
[3] E. R. Myers, P. Moorman, J. M. Gierisch, L. J. Havrilesky, L. J. Grimm, S. Ghate, et al., "Benefits and Harms of Breast Cancer Screening: A Systematic Review," JAMA. 314, 1615-34 (2015).
[4] R. E. Bird, T. W. Wallace, and B. C. Yankaskas, "Analysis of cancers missed at screening mammography," Radiology 184, 613-617 (1992).
[5] I. Andersson, D. M. Ikeda, S. Zackrisson, M. Ruschin, T. Svahn, P. Timberg, et al., "Breast tomosynthesis and digital mammography: a comparison of breast cancer visibility and BIRADS classification in a population of cancers with subtle mammographic findings," Eur. Radiol. 18, 2817-25 (2008).
[6] J. M. Park, E. A. Franken, Jr., M. Garg, L. L. Fajardo, and L. T. Niklason, "Breast tomosynthesis: present considerations and future applications," Radiographics 27, 8231-40 (2007).
[7] E. A. Rafferty, J. M. Park, L. E. Philpotts, S. P. Poplack, J. H. Sumkin, E. F. Halpem, et al., "Assessing Radiologist Performance Using Combined Digital Mammography and Breast Tomosynthesis Compared with Digital Mammography Alone: Results of a Multicenter, Multireader Trial," Radiology 266, 104-113 (2013).
[8] M. A. Durand, B. M. Haas, X. Yao, J. L. Geisel, M. Raghu, R. J. Hooley, et al., "Early clinical with digital breast tomosynthesis for screening mammography," Radiology 274, 85-92 (2015).
[9] M. M. Bonafede, V. B. Kalra, J. D. Miller, and L. L. Fajardo, "Value analysis of digital breast tomosynthesis for breast cancer screening in a commerciallyinsured US population," Clinicoecon Outcomes Res. 7, 53-63 (2015).
[10] S. P. Zuckerman, E. F. Conant, B. M. Keller, A. D. Maidment, B. Barufaldi, S. P. Weinstein, et al., "Implementation of Synthesized Two-dimensional Mammography in a Population-based Digital Breast Tomosynthesis Screening Program," Radiology 281(3), 730-736 (2016).
[11] S. A. Feig and R. E. Hendrick, "Radiation risk from screening mammography of women aged 40-49 years," J. Natl Cancer Inst. Monogr., 119-24 (1997).
[12] M. J. Yalfe and J. G. Mainprize, "Risk of radiation-induced breast cancer from mammographic screening," Radiology 258, 98-105 (2011).
[13] M. J. Yalfe, "Reducing radiation doses for breast tomosynthesis?," Lancet Oncol. 17, 1027-9 (2016).
[14] K. Dabov, R. Foi, V. Katkovnik, and K. Egiazarian, "Image Denoising by Sparse 3D Transform-Domain Collaborative Filtering," IEEE Trans. Image Process. 16, 2080-95 (2007).
[15] M. Aharon, M. Elad, and A. Bruckstein, "K-svd: An algorithm for designing overcomplete dictionaries for sparse representation," IEEE Trans. Signal Proc. 54(11), 4311–22 (2006).
[16] Suzuki K, Liu J, Zarshenas A, Higaki T, Fukumoto W, Awai K., "Neural network convolution (NNC) for converting ultra-low-dose to "virtual" high-dose CT images," LNCS: International Workshop on Machine Learning in Medical Imaging, 334–343 (2017).
[17] Suzuki K., "Overview of Deep Learning in Medical Imaging," Radiological Physics and Technology 10(3), 257-273 (2017).
[18] Suzuki, K., Horiba, I., Sugie, N., Nanki, M., "Neural filter with selection of input features and its application to image quality improvement of medical image sequences," IEICE Trans. Inf. Syst. E85-D, 1710-1718 (2002).
[19] Suzuki, K., Horiba, I., Sugie, N., "Efficient approximation of neural filters for removing quantum noise from images," IEEE Trans. Signal Process. 50, 1787-1799 (2002).
[20] Suzuki, K., Horiba, I., Sugie, N., "Neural edge enhancer for supervised edge enhancement from noisy images," IEEE Trans. Pattern Anal. Mach. Intell. 25, 1582-1596 (2003).
[21] Suzuki, K., Horiba, I., Sugie, N., Nanki, M., "Extraction of left ventricular contours from left ventriculograms by means of a neural edge detector," IEEE Trans. Med. Imaging 23, 330-339 (2004).
[22] Suzuki, K., Armato, S.G., 3rd, Li, F., Sone, S., Doi, K., "Massive training artificial neural network (MTANN) for reduction of false positives in computerized detection of lung nodules in low-dose computed tomography," Med. Phys. 30, 1602-1617 (2003).
[23] Suzuki, K., Li, F., Sone, S., Doi, K., "Computer-aided diagnostic scheme for distinction between benign and malignant nodules in thoracic low-dose CT by use of massive training artificial neural network," IEEE Trans. Med. Imaging 24, 1138-1150 (2005).

[24] Suzuki K., Yoshida H., Nappi J., and Dachman A. H."Massive-training artificial neural network (MTANN) for reduction of false positives in computer-aided detection of polyps: suppression of rectal tubes," Med. Phys. 33, 3814-3824 (2006).
[25] Suzuki, K., Yoshida, H., Nappi, J., Armato, S.G., 3rd, Dachman, A.H., "Mixture of expert 3D massive-training ANNs for reduction of multiple types of false positives in CAD for detection of polyps in CT colonography," Med. Phys. 35, 694-703 (2008).
[26] Suzuki K., "Supervised 'lesion-enhancement' filter by use of a massive-training artificial neural network (MTANN) in computer-aided diagnosis (CAD)," Physics in Medicine and Biology 54, S31-S45 (2009).
[27] Suzuki K., Rockey D. C., and Dachman A. H., "CT colonography: Advanced computer-aided detection scheme utilizing MTANNs for detection of 'missed' polyps in a multicenter clinical trial," Med. Phys. 37, 12-21 (2010).
[28] Xu, J., Suzuki, K., "Massive-training support vector regression and Gaussian process for false-positive reduction in computer-aided detection of polyps in CT colonography," Med. Phys. 38, 1888-1902 (2011).
[29] Suzuki, K., Zhang, J., Xu, J., "Massive-training artificial neural network coupled with Laplacian-eigenfunction-based dimensionality reduction for computer-aided detection of polyps in CT colonography," IEEE Trans. Med. Imaging 29, 1907-1917 (2010).
[30] Rumelhart, D.E., Hinton, G.E., Williams, R.J., "Learning representations by back-propagating errors," Nature 323, 533-536 (1986).
[31] Suzuki K., and Doi K., "How can a massive training artificial neural network (MTANN) be trained with a small number of cases in the distinction between nodules and vessels in thoracic CT?," Academic Radiology 12, 1333-1341 (2005).
[32] Wang, Z., Bovik, A.C., Sheikh, H.R., Simoncelli, E.P., "Image quality assessment: from error visibility to structural similarity," IEEE Trans. Image Proc. 13, 600-612 (2004).
[33] Tomasi, C., Manduchi, R., "Bilateral filtering for gray and color images," Sixth International Conference on Computer Vision, 839-846 (1998).